https://doi.org/10.5194/acp-2019-1138
Preprint. Discussion started: 3 February 2020

Atmospheric Chemistry and Physics Discussions

Chemical loss processes of isocyanic acid, HNCO, in the atmosphere

Simon Rosanka[1], Giang H. T. Vu[2], Hue M. T. Nguyen[2], Tien V. Pham[3], Umar Javed[1], Domenico Taraborrelli[1], Luc Vereecken[1]

[1] Institute for energy and climate research, Forschungszentrum Jülich Gmbh, Jülich, Germany
[2] Faculty of Chemistry and Centre for Computational Science, Hanoi National University of Education, Hanoi, Vietnam
[3] School of Chemical Engineering, Hanoi University of Science and Technology, Hanoi, Vietnam

Correspondence to: Hue M.T. Nguyen (hue.nguyen@hnue.edu.vn) or Domenico Taraborrelli (d.taraborrelli@fz-juelich.de)

Abstract

The impact of chemical loss processes of isocyanic acid was studied by a combined theoretical and modeling study. The potential energy surfaces of the reactions of HNCO with OH and NO_3 radicals, Cl atoms, and ozone, were studied using high-level CCSD(T)/CBS(DTQ)//M06-2X/aug-cc-pVTZ quantum chemical methodologies, followed by TST theoretical kinetic predictions of the rate coefficients at temperatures of 200-3000K. It was found that the reactions are all slow in atmospheric conditions, with $k(300K) \leq 7\times10^{-16}$ cm^3 $molecule^{-1}$ s^{-1}; the predictions are in good agreement with earlier experimental work, where available. The reverse reactions of NCO radicals, of importance mostly in combustion, were also examined briefly. The global model confirms that gas phase chemical loss of HNCO is a negligible process, contributing less than 1%. Removal of HNCO by clouds and precipitation is a larger sink, contributing for about 10% of the total loss, while globally dry deposition is the main sink, accounting for ~90%. The global simulation also shows that due to its long chemical lifetime in the free troposphere, HNCO can be efficiently transported into the UTLS by deep convection events. Average daily concentrations of HNCO are found to rarely exceed levels considered potentially toxic, though locally instantaneous toxic levels are expected.

1 Introduction

The existence of isocyanic acid (HNCO) in the atmosphere has been established only recently (Roberts et al., 2011; Wentzell et al., 2013) despite being first recognized in the 19th century (Liebig and Wöhler, 1830). HNCO can form H-bonded clusters (Zabardasti et al., 2009, 2010; Zabardasti and Solimannejad, 2007), and in concentrated/pure form appreciably polymerizes to other species, but becomes fairly stable in the presence of impurities (Belson and Strachan, 1982), such that the monomer is the near-exclusive representative especially in the gaseous phase under ambient temperature conditions (Roberts et al., 2010). The background ambient mixing ratios of HNCO vary in the range of a few pptv to tens of pptv (Young et al., 2012), while in urban regions, HNCO mixing ratio increases from tens of pptv to hundreds of pptv (Roberts et al., 2014; Wentzell et al., 2013). Peak levels can reach up to a few ppbv under the conditions impacted by direct emissions (Chandra and Sinha, 2016).

https://doi.org/10.5194/acp-2019-1138
Preprint. Discussion started: 3 February 2020

Atmospheric Chemistry and Physics Discussions

HNCO is considered a highly toxic species and has been linked to adverse health effects [(Leslie et al., 2019; Roberts et al., 2011; Suarez-Bertoa and Astorga, 2016; SUVA, 2016; Wang et al., 2007) and references therein], and human exposure to concentrations larger than 1 ppbv is considered as potentially toxic (Roberts et al., 2011). Unfortunately, an air quality standard for HNCO does not exist in most of the countries, whereas an occupational exposure limit has been established by law in only a few countries, including Sweden (SWEA, 2011) and Switzerland (SUVA, 2016). For example, the Swedish work environment authority sets the level limit value (LLV) for HNCO at about 0.018 mg m^{-3}, i.e. 10 ppbv (SWEA, 2011). The potential negative impact on health makes it important to assess the atmospheric sources and sinks of HNCO to determine its fate and lifetime.

HNCO emission into the atmosphere is driven primarily by combustion processes based on both natural and anthropogenic activities [(Leslie et al., 2019) and references therein], where the pyrolysis of nitrogen-containing biomass materials during the events of wildfires and agricultural fires leads to the emission of HNCO into the atmosphere. The presence of HNCO in the cigarette smoke has been established via the pyrolysis of urea (cigarette additive), oxidation of nicotine, and oxidation of formamide (Hems et al., 2019; Roberts et al., 2011). Even the combustion of almost all sorts of common household materials (e.g., fiber glass, rubber, foam, etc.) leads to HNCO emissions along other isocyanates [(Leslie et al., 2019) and references therein]. HNCO emissions from traffic are originating mainly from usage of recent catalytic converters in the exhaust systems of gasoline and diesel based vehicles. These converters are implemented to control the emission of primary pollutants such as hydrocarbons, carbon monoxide, particulate matter, and nitrogen oxides. However, these implementations have promoted the formation of HNCO via surface-bound chain reactions at different stages of the flue gas exhaust, and additionally due to a HNCO slippage in the most commonly used urea-based SCR (Selective Catalytic Reduction) convertion system [e.g., (Brady et al., 2014; Heeb et al., 2011; Leslie et al., 2019; Suarez-Bertoa and Astorga, 2016)]. The usages of converters in modern vehicles potentially give rise to the emission of HNCO especially in urban regions with a growing density of vehicles. A few studies also reported a direct formation of HNCO in the diesel engines during fuel combustion without any after-treatments (Heeb et al., 2011; Jathar et al., 2017). HNCO emissions via fossil fuel usage are not limited to on-road activity. Off-road fossil fuel activities (e.g., tar sands) also contribute to significant HNCO emissions on regional scales (Liggio et al., 2017). Finally, secondary HNCO formation in the atmosphere is also known through the oxidation of amines and amides [e.g., (Borduas et al., 2016a; Parandaman et al., 2017)].

The number of studies examining HNCO gas-phase chemistry is very limited, and the scarce data suggests that HNCO destruction in the atmosphere by typical pathways such as reactions with oxidizing agents or by photolysis is ineffective. We give a short overview here, to supplement a recent review (Leslie et al., 2019). The reaction of HNCO with the hydroxyl radical (OH), the most important day-time oxidizing agent, has only been studied experimentally at temperatures between 620 and 2500K (Baulch et al., 2005; Mertens et al., 1992; Tsang, 1992; Tully et al., 1989; Wooldridge et al., 1996), where the extrapolated rate expressions lead to a very low estimated rate coefficient of 5-12 × 10^{-16} cm^3 $molecule^{-1}$ s^{-1} at 298 K, i.e. a HNCO-lifetime towards OH of over 20 years when assuming a typical OH concentration of 1 × 10^6 molecule cm^{-3}. Early theoretical work by Sengupta and Nguyen (1997) at temperatures ≥ 500 K showed that the mechanism proceeds predominantly by H-abstraction, forming NCO + H_2O, with an energy barrier of ~6 kcal mol^{-1}, in agreement with the upper limit ≤

https://doi.org/10.5194/acp-2019-1138
Preprint. Discussion started: 3 February 2020

Atmospheric Chemistry and Physics Discussions

0.1 for the fraction of $CO_2 + NH_2$ formation as determined by Wooldridge et al. (1996). To our knowledge, no experimental or theoretical data are available on HNCO reactions with other dominant atmospheric oxidants, including the nitrate radical (NO_3), chlorine atoms (Cl), or ozone (O_3). Some data is available for co-reactants of importance in combustion (Baulch et al., 2005; Tsang, 1992), but these are not reviewed here. There is no direct measurement for the dry deposition of HNCO. In a recent global chemical transport model-based study, the deposition velocity was considered to be similar to formic acid, yielding an HNCO-lifetime of 1 – 3 day (over the ocean) to 1 – 2 weeks (over vegetation) (Young et al., 2012). The UV absorption for HNCO is only reported at wavelengths < 262 nm (Keller-Rudek et al., 2013; Okabe, 1970; Uno et al., 1990; Vatsa and Volpp, 2001), whereas in the troposphere photolysis occurs only at UV absorption wavelength band > 290 nm due to filtering of shorter-wavelength radiation (Hofzumahaus et al., 2002). The contribution of photolytic destruction is thus uncertain, and can only be determined by measuring HNCO absorption cross-sections directly for the relevant tropospheric wavelengths as suggested by Young et al. (2012). HNCO has absorption bands in the infra-red (Sharpe et al., 2004) but at these wavelengths generally the photon energy is too limited for photo-dissociation (Hofzumahaus et al., 2002). The main atmospheric loss processes are considered to be the transition to the liquid-phase via hydrolysis, and deposition. This process depends on the varying atmospheric liquid water contents, relevant temperatures, and pH of cloud droplets. Therefore, the gas-to-liquid partitioning, in the varying atmospheric properties, i.e. water content, temperature, and pH of cloud droplets become important parameters to determine the atmospheric fate of HNCO (Leslie et al., 2019). The gas-to-liquid partitioning has been described by the Henry's Law coefficient K_H and related parameters by a handful of studies (Borduas et al., 2016b; Roberts et al., 2011; Roberts and Liu, 2019). Based on recent studies(Barth et al., 2013; Roberts and Liu, 2019), the lifetime of HNCO due to heterogeneous processes is known to be of the order of a few hours (in-cloud reactions) to weeks (aerosol deposition).

The emissions and sources of HNCO have been focused on by many past studies, but there remain large uncertainties in our understanding of HNCO removal process, especially in gas-phase chemistry. The limited number of available studies suggests that the (photo)chemical HNCO loss processes in the atmosphere appear to be slow, with liquid-phase processes acting as the dominant sink. To alleviate the dearth of direct data, we provide in this work a theoretical analysis of the chemical reactions of HNCO with the dominant atmospheric oxidants: OH and NO_3 radicals, Cl atoms, and O_3 molecules, predicting the rate coefficients of these reactions at atmospheric conditions. The results are included in a global numerical chemistry and climate model to assess the impact of chemical loss of HNCO in competition against hydrolysis within cloud droplets and against deposition to the Earth's surface. The model is also used to provide an estimate of the relative importance of primary and secondary HNCO sources.

2 Methodologies

2.1 Theoretical methodologies

The potential energy surfaces of the initiation reactions of all four reaction systems were characterized at the M06-2X/aug-cc-pVTZ level of theory (Dunning, 1989; Zhao and Truhlar, 2008), optimizing the geometries and rovibrational characteristics of all minima and transition states. The relative energy of the critical points was

https://doi.org/10.5194/acp-2019-1138
Preprint. Discussion started: 3 February 2020

Atmospheric Chemistry and Physics Discussions

further refined at the CCSD(T) level of theory in a set of single point energy calculations using a systematic series of basis sets, aug-cc-pVxZ (x = D, T, Q) (Dunning, 1989; Purvis and Bartlett, 1982). These energies were extrapolated to the complete basis set limit (CBS) using the aug-Schwartz6(DTQ) scheme as proposed by Martin (1996). The rate coefficients were then obtained by transition state theory (Truhlar et al., 1996) in a rigid rotor, harmonic oscillator approximation, applying a scaling factor of 0.971 to the vibrational wavenumbers (Alecu et al., 2010; Bao et al., 2017). The spin-orbit splitting of the OH radicals of 27.95 cm^{-1} was taken into account (Huber and Herzberg, 1979). Tunneling was incorporated using an asymmetric Eckart correction (Johnston and Heicklen, 1962). The expected uncertainty of the predictions at room temperature is a factor of 4, based on an estimated uncertainty on the barrier height of 0.5 kcal mol^{-1}, and on the tunneling correction of a factor of 1.5.

To further complete our knowledge on some of the reactions beyond their initiation steps, the full potential energy surfaces of the HNCO + Cl and HNCO + O_3, were characterized at the M06-2X/aug-cc-pVTZ or B3LYP/aug-cc-pVTZ level of theory (Becke, 1993; Dunning, 1989; Lee et al., 1988), combined with CCSD(T)/aug-cc-pVTZ single point energy calculations. To our knowledge, these are the first characterizations of these surfaces. At atmospheric temperatures, most of the reaction channels are negligible, and a detailed kinetic analysis is not performed at this time.

2.2 Global modeling

The ECHAM/MESSy Atmospheric Chemistry (EMAC) model is a numerical chemistry and climate simulation system that includes sub-models describing tropospheric and middle atmosphere processes and their interaction with oceans, land and human influences (Jöckel et al., 2010). It uses the second version of the Modular Earth Submodel System (MESSy2) to link multi-institutional computer codes. The core atmospheric model is the 5th generation European Centre Hamburg general circulation model (ECHAM5) (Roeckner et al., 2006). For the present study we applied EMAC (ECHAM5 version 5.3.02, MESSy version 2.54.0) in the T63L90MA-resolution, i.e. with a spherical truncation of T63 (corresponding to a quadratic Gaussian grid of approximately 1.875 by 1.875 degrees in latitude and longitude) with 90 vertical hybrid pressure levels up to 0.01 hPa. The applied model setup comprised the submodel MECCA (Module Efficiently Calculating the Chemistry of the Atmosphere) to calculate atmospheric chemistry using parts of the Mainz Organic Mechanism (MOM) (Sander et al., 2011), excluding aromatics and terpenes. The mechanism was extended to include the proposed changes of this study, formamide as an additional chemical source of isocyanic acid (Bunkan et al., 2016), and chemical mechanisms for nitromethane (Calvert, 2008; Taylor et al., 1980), methylamine, dimethylamine and trimethylamine (Nielsen et al., 2012). The submodel SCAV (SCAVenging submodel) was used to simulate the removal of trace gases and aerosol particles by clouds and precipitation (Tost et al., 2006). The aqueous phase mechanism was extended to include the isocyanic acid and formamide mechanism proposed by Borduas et al. (2016b), Barnes et al. (2010), and Behar (1974). The representation of cyanide was improved based on Buechler et al. (1976). Table 1 and 2 in the supplementary material summaries all additional changes to the chemical mechanism in gas and aqueous phase, respectively. The major sources of isocyanic acid and formamide are biomass burning emissions. From literature two emission factors are available (Koss et al., 2018; Kumar et al., 2018) which differ substantially. Thus two simulations are performed, to quantify the uncertainty in those

https://doi.org/10.5194/acp-2019-1138
Preprint. Discussion started: 3 February 2020

Atmospheric Chemistry and Physics Discussions

emission factors. The MESSy submodel BIOBURN is used to calculate biomass burning fluxes based on the selected emission factor and Global Fire Assimilation System (GFAS) data. GFAS data are calculated based on fire radiative power observations from Moderate Resolution Imaging Spectroradiometer (MODIS) satellite instruments, which are used to calculate the dry matter combustion rates (Kaiser et al., 2012). The biomass burning emission fluxes are then obtained by combining these dry matter combustion rates with the defined biomass burning emission factors per unit of dry matter burned. The MESSy submodel OFFEMIS (OFFLine Emissions) then calculates the resulting concentration changes for each tracer due to the biomass burning emissions (Kerkweg et al., 2006). Anthropogenic isocyanic acid emission from diesel cars are scaled to ammonia EDGAR (Crippa et al., 2016) road emission by 15% (Heeb et al., 2011). The model was run for two years (2010-2011) in which the first year was used as spin up and 2011 for analysis.

3 Loss processes by chemical oxidants

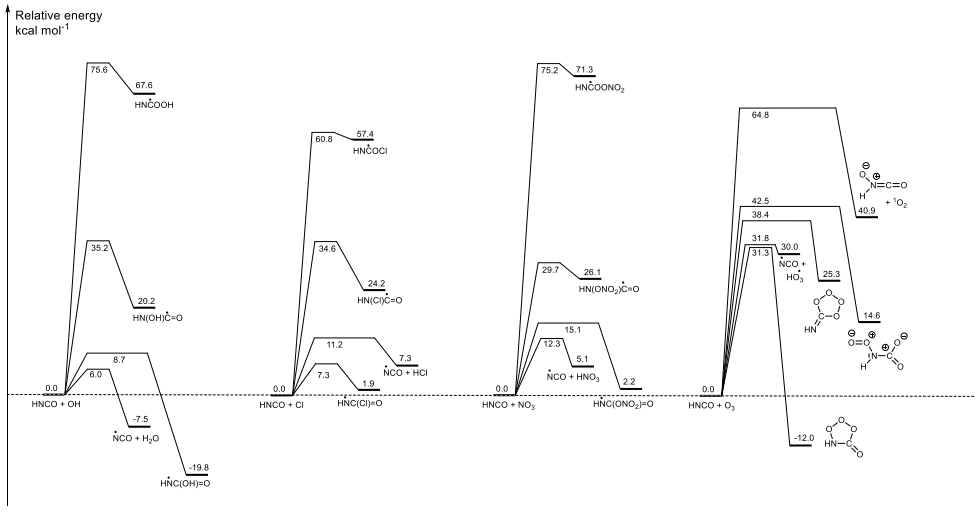

Figure 1: Potential energy surfaces for the initiation reactions of isocyanic acid (HNCO) with OH radicals, Cl atoms, NO_3 radicals, and ozone, showing CCSD(T)/CBS(DTQ) energies (kcal mol^{-1}) based on M06-2X/aug-cc-pVTZ geometries. The supporting information has complete surfaces for some of the reactions.

3.1 HNCO + OH

The reaction of isocyanic acid with OH can proceed by 4 distinct pathways: H-abstraction, or OH addition on the carbon, nitrogen, or oxygen atom of HNCO; a potential energy surface is shown in Figure 1. Formation of the HN=C$^{\bullet}$OOH and HN(OH)C$^{\bullet}$=O adducts through OH-addition on the oxygen or nitrogen atom is highly endothermic by 20 kcal mol^{-1} or more, and is not competitive at any temperature. The two remaining pathways are exothermic, with HN$^{\bullet}$C(=O)OH being the most stable nascent product, 20 kcal mol^{-1} below the reactants, followed by H_2O + $^{\bullet}$N=C=O, at 7.5 kcal mol^{-1} exoergicity. Despite the higher energy of the products, we predict this latter reaction to have a lower barrier, 6 kcal mol^{-1}, compared to the addition process, 9 kcal mol^{-1}, in

https://doi.org/10.5194/acp-2019-1138
Preprint. Discussion started: 3 February 2020

Atmospheric Chemistry and Physics Discussions

agreement with the theoretical predictions of Sengupta and Nguyen (1997). Furthermore, the H-abstraction process allows for faster tunneling, making this process the fastest reaction channel, while addition contributes less than 0.5% of product formation at temperatures below 400K. From this data, we derive the following rate coefficient expressions (see also Figure 2):

$k_{OH}(298K) = 7.03\times10^{-16}$ cm^3 molecule^{-1} s^{-1}

$k_{OH}(200\text{-}450K) = 3.27\times10^{-34}\ T^{7.01}\ \exp(685K/T)$ cm^3 molecule^{-1} s^{-1}

$k_{OH}(300\text{-}3000K) = 1.79\times10^{-23}\ T^{3.48}\ \exp(-733K/T)$ cm^3 molecule^{-1} s^{-1}

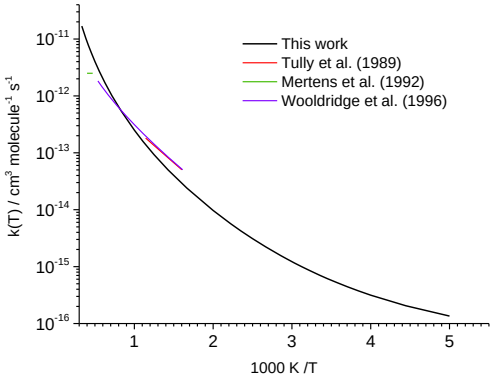

Figure 2: Predicted rate coefficient k(T) for the reaction of HNCO + OH, compared against experimental data.

Our predictions are in very good agreement between 624-875K, when compared with experimental data from Tully et al. (1989), which served as the basis for the recommendation of Tsang (1992); our predictions reproduce the rate coefficients within a factor 1.7, comparable to the experimental uncertainty of a factor 1.5 (see Figure 2). Likewise, our predictions agree within a factor 1.7 with the experimental determination of Wooldridge et al. (1996), over the entire 620-1860 K temperature range. Our predictions overshoot the upper limit estimated by Mertens et al. (1992) by a factor of up to 4 at the upper end of the temperature range (2120 to 2500 K). At these elevated temperatures, it is expected that our kinetic model is less accurate since anharmonicity, internal rotation, and possibly pressure effects are not fully accounted for. At this time, we choose not to invest the computational cost to improve the model at these temperatures. The predicted rate at room temperature is within a factor of 2 of the extrapolation of the recommended expression derived by Tsang (1992), k(298 K) $\approx 1.24\times10^{-15}$ cm^3 molecule^{-1} s^{-1}, and very close to the extrapolation of the expression by Wooldridge et al. (1996), 7.2×10^{-16} cm^3 molecule^{-1} s^{-1}. The good agreement of our rate coefficient with the experimental data extrapolated to room temperature is mainly due to the curvature predicted in the temperature-dependence (see Figure 2), as our calculations have a slightly steeper temperature dependence than the experiments in the high-temperature range. Though negligible at low temperature, , we find that OH addition on the C-atom of HNCO accounts for 7 to 8 % of the reaction rate between 2000 and 3000 K, with other non-H-abstraction channels remaining negligible (<0.1%).

Typical concentrations of the OH radical during daytime are measured at ~10^6 molecule cm^{-3} (Stone et al., 2012), leading to an pseudo-first order rate coefficient for HNCO loss by OH radicals of k(298K) = 10^{-10} s^{-1}, i.e.

https://doi.org/10.5194/acp-2019-1138
Preprint. Discussion started: 3 February 2020

Atmospheric Chemistry and Physics Discussions

a chemical lifetime of several decades, negligible compared to other loss processes like scavenging. Even in extremely dry conditions, where aqueous uptake is slow, heterogeneous loss processes will dominate, or alternatively atmospheric mixing processes will transport HNCO to more humid environments where it will hydrolyze.

3.2 HNCO + Cl

From the potential energy surface (PES) shown in Figure 1, we see that the reaction between HNCO and Cl atom can occur by abstraction of the H atom from HNCO, or by addition of the Cl atom on the C-, N- or O-atoms. Contrary to the OH-reaction, all entrance reactions are endothermic, with formation of the HN•C(Cl)=O alkoxy radical nearly energy-neutral (see Figure 1). Formation of this latter product, proceeding by the addition of a Cl atom to the carbon atom of HNCO, also has the lowest energy barrier, 7 kcal mol^{-1} above the reactants. The hydrogen abstraction, forming HCl and •NCO, requires passing a higher barrier of 11 kcal mol^{-1}, whereas addition on the N- and O-atoms have very high barriers exceeding 34 kcal mol^{-1}. The product energy difference between addition and H-abstraction is much smaller compared to the HNCO + OH reaction, because of the absence of the stabilizing effect of the –COOH functionality in the Cl-adduct. Despite this, the addition barrier remains 4 kcal mol^{-1} below the H-abstraction barrier, making the HNCO + Cl reaction the only reaction studied here where H-abstraction is not dominant. For the HNCO + Cl reaction, we then obtain the following rate coefficients (see also Figure 3):

$$k_{Cl}(298K) = 3.19\times10^{-17}\ cm^3\ molecule^{-1}\ s^{-1}$$

$$k_{Cl}(200\text{-}450K) = 1.11\times10^{-17}\ T^{1.97}\ \exp(-3031K/T)\ cm^3\ molecule^{-1}\ s^{-1}$$

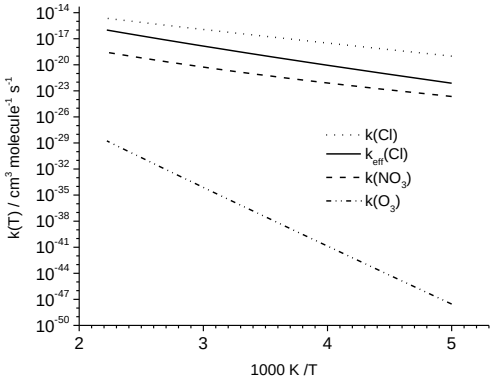

Figure 3: Total rate coefficient predictions for the reaction of HNCO with NO_3, Cl and O_3. The addition of Cl atoms on HNCO leads to the formation of a very short-lived adduct, which rapidly redissociates to the reactants; the effective rate coefficient for HNCO loss by Cl atoms, $k_{eff}(Cl)$, is thus equal to the H-abstraction rate forming HCl + NCO.

We find that the overall rate coefficient of the HNCO + Cl reaction is almost one order of magnitude below that for the OH radical. The HN•C(Cl)=O radical formed, however, has a weak C–Cl bond requiring only 5.4 kcal mol^{-1} to redissociate. The rate coefficient of $8\times10^8\ s^{-1}$ for dissociation at room temperature ($k(T) = 8.3\times10^{12}$

https://doi.org/10.5194/acp-2019-1138
Preprint. Discussion started: 3 February 2020

Atmospheric Chemistry and Physics Discussions

exp(-2760/T) s^{-1}), makes redissociation to the reactants the most likely fate of the HN•C(Cl)=O adduct. Addition is thus an ineffective channel for HNCO removal, and the effective reaction with Cl atoms is dominated by the H-abstraction reaction, forming HCl + •NCO, with the following rate coefficient (see also Figure 3):

$$k_{Cl,eff}(298K) = 2.23\times10^{-19}\ cm^3\ molecule^{-1}\ s^{-1}$$

$$k_{Cl,eff}(200\text{-}450K) = 1.01\times10^{-24}\ T^{4.40}\ exp(-3799\ K/T)\ cm^3\ molecule^{-1}\ s^{-1}$$

Globally, Cl atoms have a lower concentration, about 5×10^3 atom cm^{-3}, compared to OH radicals (Finlayson-Pitts and Pitts, 1999). Under such conditions, lifetimes estimated for HNCO towards Cl atoms are about 3×10^7 years, which is much longer than toward the OH radial. Therefore, HNCO loss by Cl radicals is negligible.

The supporting information provides information on the extended potential energy surface of the HNCO + Cl reaction, with information on 9 intermediates, 19 transition states, and 16 products.

3.3 HNCO + NO_3

The reaction of NO_3 with HNCO shows the same four radical mechanisms found for OH and Cl, i.e. H-abstraction and addition on the 3 heavy atoms. As for Cl-atoms, none of the reactions are exothermic, and the energy difference between the two most stable products, is reduced to 3 kcal mol^{-1}, indicating that NO_3 addition is even less favorable than Cl addition. Formation of HNO_3 + •NCO is more favorable than HCl + NCO formation, by about 2 kcal mol^{-1}, owing to the greater stability of nitric acid. The barrier for H-abstraction, however, is larger compared to abstraction by both OH and Cl, and exceeds 12 kcal mol^{-1}. The most favorable addition process, forming HN•C(=O)NO_3 has a barrier of 15 kcal mol^{-1}, but contributes less than 0.01% to the reaction rate at room temperature. The overall reaction thus proceeds near-exclusively by H-abstraction forming HNO_3 + •NCO, for which we derived the following rate coefficients (see also Figure 3):

$$k_{NO3}(298K) = 1.11\times10^{-21}\ cm^3\ molecule^{-1}\ s^{-1}$$

$$k_{NO3}(200\text{-}450K) = 8.87\times10^{-42}\ T^{9.06}\ exp(-1585K/T)\ cm^3\ molecule^{-1}\ s^{-1}$$

While this rate coefficient is almost 5 orders of magnitude below that of the OH radical, the nitrate radical is known to be present in higher concentrations during night time, reaching concentrations as high as 10^9 molecule cm^{-3} (Finlayson-Pitts and Pitts, 1999). The effective rate of the NO_3 reaction at night time is similar to the reaction with OH at day time. The NO_3 radical is thus still considered to be ineffective for atmospheric removal of HNCO.

3.4 HNCO + O_3

The chemistry of ozone with organic compounds is drastically different from radicals, where O_3 typically reacts by cycloaddition on double bonds in unsaturated compounds. For isocyanic acid, cycloaddition pathways have been characterized for both double bonds (HN=C=O). Only cycloaddition on the N=C bond leads to an exothermic reaction, with the oxo-ozonide product being 12 kcal mol^{-1} more stable than the reactants (see Figure 1). In addition to the traditional cycloaddition channels, three further channels were found, corresponding to H-abstraction, forming HO_3 + NCO, oxygen transfer to the N-atom, forming ON(H)CO + $^1O_2$, and addition on the C- and N-atom, forming HN(OO)C(O)O. The HO_3 product radical is known to be only weakly bonded by 2.94 kcal mol^{-1}, falling apart to OH + O_2 (Bartlett et al., 2019; Le Picard et al., 2010; Varandas, 2014).

https://doi.org/10.5194/acp-2019-1138
Preprint. Discussion started: 3 February 2020

Atmospheric Chemistry and Physics Discussions

The cyclo-addition channels on the hetero-double bonds have high energy barriers, exceeding 30 kcal mol^{-1}, significantly larger than typical barriers for C=C bonds with aliphatic substitutions. Surprisingly, this allows H-abstraction to become competitive to cycloaddition, with a comparable barrier of 32 kcal mol^{-1}. For the overall reaction, we obtain the following rate coefficients (see also Figure 3):

$$k_{O3}(298K) = 2.95\times10^{-37}\ cm^3\ molecule^{-1}\ s^{-1}$$

$$k_{O3}(200\text{-}450K) = 3.72\times10^{-23}\ T^{2.96}\ \exp(-14707K/T)\ cm^3\ molecule^{-1}\ s^{-1}$$

At room temperature, H-abstraction contributes 80% to the total reaction, and cycloaddition on the N=C bond the remaining 20%. All other channels are negligible. The rate coefficient is exceedingly low, $\sim10^{-37}$ cm^3 $molecule^{-1}$ s^{-1}, such that even in areas with very high ozone concentrations of 100 ppbv the loss by ozonolysis is expected to be negligible.

The supporting information provides information on the extended potential energy surface of the HNCO + O_3 reaction, with information on 10 intermediates, 30 transition states, and 15 products. The lowest-energy unimolecular product channel leads to formation of CO_2 + HNOO by breaking of the cyclic primary ozonide (see Figure 1) following the traditional Criegee mechanism (Criegee, 1975).

4 Global impact

From our global simulations, we gain many insights on the impact of the described mechanism (Table 1 and 2 in the supplementary material) under atmospheric conditions. Figure 4 shows the mean seasonal surface mixing ratio of isocyanic acid using the biomass burning emission factors by Koss et al. (2018). It can be observed that high levels persist in each season. In general, high HNCO levels occur in regions associated with frequent biomass burning activities. Regions with no biomass burning activities have low HNCO concentrations, mainly caused by free tropospheric entrainment from regions with higher concentrations. This becomes evident when taking into account that the free troposphere contains about 81% of the total HNCO mass.

Table 1 shows the corresponding HCNO budget for both performed simulations. The gas-phase production via formamide differs greatly in relation to the biomass burning emissions used. In the case of Kumar et al. (2018), significantly more formamide is emitted, leading to a higher production of isocyanic acid in the gas phase. Gas phase chemical losses of HNCO are small, with only the reaction of HNCO with OH leading to some destruction of HNCO, while the other chemical sinks (O_3, NO_3 and Cl) are negligible. When compared to the major loss processes, however, all these loss processes are on a global scale negligible. The major sinks are dry deposition and scavenging (heterogeneous losses), where the latter contributes 274.60 and 377.19 Gg/year when using the emission factors by Koss et al. (2018) and Kumar et al. (2018), respectively. Therefore, it can be concluded that the gas-phase chemical sinks analysed in this study (OH, Cl, NO_3, O_3) can be considered to be insignificant when compared to heterogeneous loss processes. This is independent of the high uncertainty in the available biomass burning emission factors or missing road emission datasets. The results in this study are in a similar order as the modelling study by Young et al. (2012). These authors have lower total HNCO emissions and do not include formamide as a secondary source of HNCO. They still have a higher chemical loss via OH, which is due to a higher rate constant used. The lifetime is still higher due to generally lower heterogeneous loss terms.

https://doi.org/10.5194/acp-2019-1138
Preprint. Discussion started: 3 February 2020

Atmospheric Chemistry and Physics Discussions

The atmospheric lifetime of HNCO is dominated by its heterogeneous loss processes, leading to an atmospheric lifetime of multiple weeks, whereasthe gas-phase lifetime in the free troposphere is about 50 years. This long gas-phase lifetime and the fact that mainly surface sources are relevant indicate that atmospheric HNCO is highly impacted by transport processes. Our simulations show that HNCO is transported from the surface into the UTLS (upper troposphere/lower stratosphere) and that about 10% of the total atmospheric HNCO mass is located in the stratosphere, with modelled concentrations of HNCO in the lower stratosphere of typically tens of pptv but reaching up to hundred pptv in tropical regions. Since OH is the only significant stratospheric sink, the stratospheric lifetime increases to more than 330 years. During the monsoon period, the total stratospheric HNCO mass increases from 15.04 Gg before to 19.75 Gg at the end of monsoon season. Pumphrey et al. (2018) demonstrated that in 2015 and 2016, elevated levels of stratospheric hydrogen cyanide (HCN) can be linked to biomass burning emissions from Indonesian fires. Similar to HNCO in our simulations, stratospheric concentrations of HCN increase during the Indian monsoon period. In the performed simulations, the ratio between stratospheric HCN and HNCO is very similar throughout the year, indicating that HCN and HNCO are similarly affected by transport processes within this period. The combination of strong biomass burning events and strong vertical transport during the monsoon period leads to high HNCO concentrations in the UTLS, indicating that pollutants from biomass burning events could potentially influence stratospheric chemistry.

Figure 5 shows the number of days exceeding a daily mean HNCO concentration of 1 ppbv. Mainly regions impacted by biomass burning events have frequent concentration above this threshold. When using 10 ppbv as limit for toxic concentrations of HNCO, as proposed by the Swedish work environment authority (SWEA, 2011), only a few days can be observed in which this limit is exceeded. The maximum number of days exceeding 10 ppbv is 10 days over Africa, compared to 120 days above 1 ppbv. It is important to take into account that this analysis is limited by the computational output available in this study, which has only daily averages. Therefore, it is expected that areas which frequently exceed daily averages of 1 ppbv are potentially areas in which peak HNCO can be observed above 10 ppbv throughout the day.

No correlation exists between the number of days exceeding 1 or 10 ppbv and road traffic emissions. This becomes evident since typical areas of high road traffic activities (i.e. USA and Europe) do not exceed daily averages of 1 ppbv (see Figure 5). Road traffic activities occur on a smaller spatial scale than biomass burning events. The EMAC model used is not capable to represent, for example, inner city road traffic activities, due to the spatial resolution of the model used (1.875 by 1.875 degrees in latitude and longitude). Therefore, we are not capable to draw any conclusion if 10 ppbv is exceeded regionally in densely populated areas, impacted by high traffic emissions.

https://doi.org/10.5194/acp-2019-1138
Preprint. Discussion started: 3 February 2020

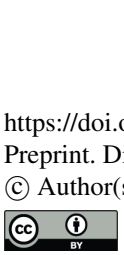

Atmospheric Chemistry and Physics Discussions

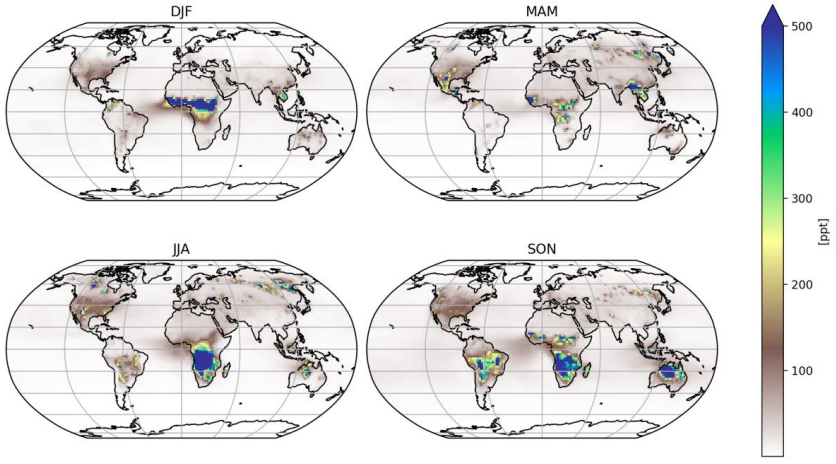

Figure 4: Mean seasonal surface concentration of isocyanic acid using Koss et al. (2018) biomass burning emission factors.

Table 1: Yearly global isocyanic acid budget in 2011 for both biomass burning emission datasets by Kumar et al. (2018) and Koss et al. (2018). Additionally, the HNCO budget from Young et al. (2012) is given for comparison.

	Koss et al., 2018	Kumar et al., 2018	Young et al., 2012
Emissions [Gg/year]			
Biomass burning (HNCO)	2158.94	814.69	661.00
Anthropogenic (HNCO)	177.14	177.14	828.00
Gas phase production [Gg/year]			
NH_2CHO + OH	482.52[a]	2365.53[b]	-
Gas phase loss [Gg/year]			
HNCO + OH	3.98	5.41	~ 5.96
HNCO + O_3	1.88×10^{-16}	2.37×10^{-16}	-
HNCO + NO_3	1.15×10^{-4}	1.43×10^{-4}	-
HNCO + Cl	9.99×10^{-8}	1.37×10^{-7}	-
Heterogeneous losses [Gg/year]			
Dry deposition	2519.61	2891.85	~ 1421.99
Scavenging	274.60	377.19	-
Wet deposition	0.13	0.16	~ 67.01
Yearly mean burden [Gg]	201.15	271.94	~ 150.00
Atmospheric lifetime [days]	26.24	30.31	36.62

[a] Of which 50.59 Gg/year NH_2CHO biomass burning emissions (Koss et al., 2018)

[b] Of which 2335.01 Gg/year NH_2CHO biomass burning emissions (Koss et al., 2018)

https://doi.org/10.5194/acp-2019-1138
Preprint. Discussion started: 3 February 2020

Atmospheric Chemistry and Physics Discussions

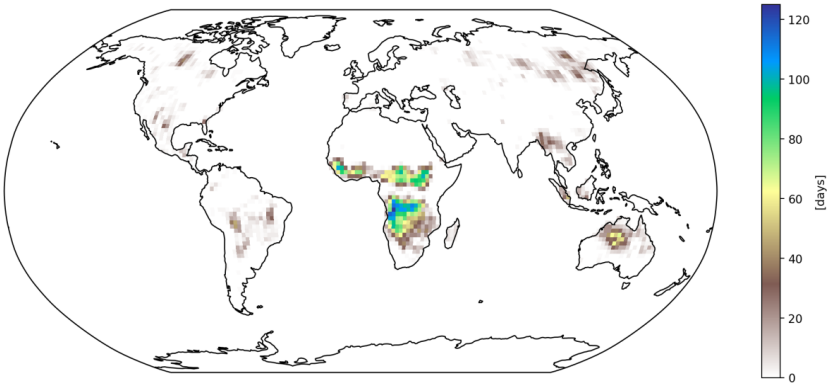

Figure 5: Number of days exceeding 1 ppb of isocyanic acid at the surface. Biomass burning emission factors are based on Koss et al. (2018)

5 H-abstraction reactions by NCO radicals

The radical reactions characterized above proceed by H-abstraction, forming the NCO radical with an H_2O, HNO_3, or HCl co-product. Likewise, the ozonolysis reaction proceeds for a large part by H-abstraction, forming NCO with a HO_3 coproduct that readily dissociates to OH + O_2. Though NCO radical formation through these reactions is found to be negligibly slow in atmospheric conditions, this radical remains of interest in other environments. Examples include combustion chemistry, where it can be formed directly from nitrogen-containing fuels, and where it is a critical radical intermediate in e.g. the RAPRENOx nitrogen-oxide mitigation strategy (Fenimore, 1971; Gardiner, 2000). The NCO radical has also been observed in space (Marcelino et al., 2018). There is extensive experimental and theoretical information of the reactions of NCO radicals, tabulated e.g. in Tsang (1992), Baulch et al. (2005) and other works. To our knowledge, the rate coefficients of the reactions of NCO radicals with H_2O, HNO_3, and HCl have not been determined before, though Tsang (1992) has estimated a rate coefficient $k(NCO + H_2O) = 3.9\times10^{-19}\ T^{2.1}\ \exp(-3046K/T)$ cm^3 $molecule^{-1}$ s^{-1} based on the equilibrium constant and rate coefficient of the HNCO + OH reaction. Since the H–N bond in HNCO is quite strong, with a bond energy of ~110 kcal/mol (Ruscic, 2014; Ruscic and Bross, 2019), it is expected that NCO can readily abstract a hydrogen atom from most hydrogen-bearing species to produce HNCO, and that H-abstraction is the main reaction channel. Hence, despite that our potential energy surfaces do not include an exhaustive search of the NCO radical chemistry, we expect that predictions of the H-abstraction rate for NCO from H_2O, HNO_3 and HCl are fair estimates of the total rate coefficients of these reactions.

The energy barriers for the NCO radical reactions with H_2O, HNO_3 and HCl, being 14, 7, and 4 kcal mol^{-1} respectively (see Figure 1), follow the bond strength trend in these reactants, with D_0(H–OH) = 118 kcal mol^{-1}, D_0(H–NO_3) = 104 kcal mol^{-1}, and D_0(H–Cl) = 103 kcal mol^{-1} (Luo, 2007; Ruscic et al., 2002). Figure 1 also shows that the NCO + H_2O reaction is endothermic by 8 kcal mol^{-1}, while the HNO_3 and HCl paths are exothermic by -5 and -7 kcal mol^{-1}, respectively. The predicted rate coefficients are then:

$$k_{NCO+H2O}(300K) = 1.36\times10^{-21}\ cm^3\ molecule^{-1}\ s^{-1}$$

$$k_{NCO+HNO3}(300K) = 3.37\times10^{-17}\ cm^3\ molecule^{-1}\ s^{-1}$$

https://doi.org/10.5194/acp-2019-1138
Preprint. Discussion started: 3 February 2020

Atmospheric Chemistry and Physics Discussions

$k_{NCO+HCl}(300K) = 1.39\times10^{-14}$ cm^3 molecule^{-1} s^{-1}

$k_{NCO+H2O}(300\text{-}3000K) = 4.59\times10^{-24}\ T^{3.63}\ \exp(-4530K/T)$ cm^3 molecule^{-1} s^{-1}

$k_{NCO+HNO3}(300\text{-}3000K) = 7.18\times10^{-26}\ T^{4.21}\ \exp(-1273K/T)$ cm^3 molecule^{-1} s^{-1}

$k_{NCO+HCl}(300\text{-}3000K) = 3.73\times10^{-20}\ T^{2.63}\ \exp(-662K/T)$ cm^3 molecule^{-1} s^{-1}

The indirect estimate of Tsang (1992) compares well to our prediction for NCO + H_2O, reproducing our values within a factor 15 at 1000K and factor 3 at 2000K, i.e. within the stated uncertainties. An analysis of the impact of the NCO reactions in combustion or non-terrestrial environments is well outside the scope of this paper, and reactions with other co-reactants not discussed in this paper are likely to be of higher importance, e.g. H-abstraction from organic compounds, or recombination with other radicals. In atmospheric conditions, the fate of the NCO radical is likely recombination with an O_2 molecule, leaving H_2O, HNO_3, and HCl as negligible co-reactants. Hence, the NCO radical will not affect the atmospheric fate of any of these compounds to any extent. Subsequent chemistry of the •OONCO radical is assumed to be conversion to an •ONCO alkoxy radical through reactions with NO, HO_2 or RO_2, followed by dissociation to NO + CO.

6 Conclusions

The isocyanic acid molecule, HNCO, is found to be chemically fairly unreactive towards the dominant atmospheric gas phase oxidants, i.e. OH and NO_3 radicals, Cl atoms, and O_3 molecules. The reactions all occur predominantly by H-abstraction, and have comparatively low rates of reactions with $k(298) \leq 7\times10^{-16}$ cm^3 molecule^{-1} s^{-1}, leading to chemical gas phase lifetimes of decades. Yearly loss of HNCO towards these reactants is ~5 Gg/y. Removal of HNCO by clouds and precipitation ("scavenging"), leading to hydrolysis to ammonia, is also implemented in the global model, and was found to contribute significantly more, ~300 Gg/y, than the gas phase loss processes. Still, these combined processes are overwhelmed by the loss of HNCO by dry deposition, removing ~2700 Gg/y. These conclusions are robust against modifications of the emission scenarios, where two distinct sets of emission factors were used, incorporating HNCO formation from biomass burning, as well as anthropogenic sources such as formamide oxidation and road traffic. The inefficiency of gas-phase chemical loss processes confirms earlier assumptions; inclusion of the gas-phase chemical loss processes in kinetic models appears superfluous except in specific experimental conditions with very high co-reactant concentrations. The long gas-phase chemical lifetime (multiple decades) allows HNCO to be transported efficiently into the UTLS demonstrating that surface emissions may impact the upper troposphere. Further research is necessary to identify the importance of strong biomass burning events coupled to strong vertical transport processes (i.e. monsoon systems) on the chemical composition of the UTLS.

On a global scale, the daily average concentrations of HNCO rarely exceed 10 ppbv, the threshold assumed here for toxicity; the exceedances are mainly located in regions with strong biomass burning emissions. Average daily concentrations of the order of 1 ppbv are encountered more frequently, with about 1/3th of the year exceeding this limit. This suggests that local concentrations might peak to much higher values, e.g. in urban environments where road traffic emissions are highest, or in the downwind plume of biomass burning events, and could impact regional air quality. Such regional effects were not studied in the current work, as the resolution of the global model used here is not sufficiently fine-grained.

https://doi.org/10.5194/acp-2019-1138
Preprint. Discussion started: 3 February 2020

Atmospheric Chemistry and Physics Discussions

Though not important for the atmosphere, we briefly examined the reactions of the NCO radical formed in the chemical reactions studied. The rate coefficients of the H-abstraction reactions with H_2O, HNO_3 and HCl suggest that these reactions might contribute in high-temperature environments, such as combustion processes.

Supplement

The supplement related to this article is available online, and contains extended information on the chemical model, and the quantum chemical characterizations (geometric, energetic and entropic data)

Author contributions

The quantum chemical calculations where performed by H.M.T. Nguyen, G.H.T. Vu, and T.V. Pham, while L. Vereecken performed the theoretical kinetic calculations. U. Javed, S. Rosanka and D. Taraborrelli collected the literature data on HNCO sources and sinks, and implemented these in the kinetic model; the model runs were performed by S. Rosanka and D. Taraborrelli. All authors contributed significantly to the writing of the manuscript.

Competing interests

The authors declare that they have no conflict of interest.

Acknowledgments

HMTN, GHTV and TVP thank the National Foundation for Science and Technology Development (Nafosted), Vietnam for sponsoring this work under project number 104.06-2015.85. SR and DT gratefully acknowledge the Earth System Modelling Project (ESM) for funding this work by providing computing time on the ESM partition of the supercomputer JUWELS at the Jülich Supercomputing Centre (Forschungszentrum Jülich, 2019).

References

Alecu, I. M., Zheng, J., Zhao, Y. and Truhlar, D. G.: Computational Thermochemistry: Scale Factor Databases and Scale Factors for Vibrational Frequencies Obtained from Electronic Model Chemistries, J. Chem. Theory Comput., 6(9), 2872–2887, doi:10.1021/ct100326h, 2010.

Bao, J. L., Zheng, J., Alecu, I. M., Lynch, B. J., Zhao, Y. and Truhlar, D. G.: Database of Frequency Scale Factors for Electronic Model Chemistries (Version 3 Beta 2), [online] Available from: http://comp.chem.umn.edu/freqscale/index.html, 2017.

Barnes, I., Solignac, G., Mellouki, A. and Becker, K. H.: Aspects of the Atmospheric Chemistry of Amides, Chemphyschem, 11(18), 3844–3857, doi:10.1002/cphc.201000374, 2010.

https://doi.org/10.5194/acp-2019-1138
Preprint. Discussion started: 3 February 2020

Atmospheric Chemistry and Physics Discussions

1 Barth, M. C., Cochran, A. K., Fiddler, M. N., Roberts, J. M. and Bililign, S.: Numerical modeling of cloud
2 chemistry effects on isocyanic acid (HNCO), J. Geophys. Res.-Atmospheres, 118(15), 8688–8701,
3 doi:10.1002/jgrd.50661, 2013.

4 Bartlett, M. A., Kazez, A. H., Schaefer, H. F. and Allen, W. D.: Riddles of the structure and vibrational
5 dynamics of HO_3 resolved near the ab initio limit, J. Chem. Phys., 151(9), 094304, doi:10.1063/1.5110291,
6 2019.

7 Baulch, D. L., Bowman, C. T., Cobos, C. J., Cox, R. A., Just, Th., Kerr, J. A., Pilling, M. J., Stocker, D., Troe,
8 J., Tsang, W., Walker, R. W. and Warnatz, J.: Evaluated Kinetic Data for Combustion Modeling: Supplement II,
9 J. Phys. Chem. Ref. Data, 34(3), 757, doi:10.1063/1.1748524, 2005.

10 Becke, A. D.: A New Mixing of Hartree-Fock and Local Density-Functional Theories, J. Chem. Phys., 98(2),
11 1372–1377, doi:10.1063/1.464304, 1993.

12 Behar, D.: Pulse-Radiolysis Study of Aqueous Hydrogen-Cyanide and Cyanide Solutions, J. Phys. Chem.,
13 78(26), 2660–2663, doi:10.1021/j100619a005, 1974.

14 Belson, D. J. and Strachan, A. N.: Preparation and Properties of Isocyanic Acid, Chem. Soc. Rev., 11(1), 41–56,
15 doi:10.1039/cs9821100041, 1982.

16 Borduas, N., Murphy, J. G., Wang, C., da Silva, G. and Abbatt, J. P. D.: Gas Phase Oxidation of Nicotine by OH
17 Radicals: Kinetics, Mechanisms, and Formation of HNCO, Environ. Sci. Technol. Lett., 3(9), 327–331,
18 doi:10.1021/acs.estlett.6b00231, 2016a.

19 Borduas, N., Place, B., Wentworth, G. R., Abbatt, J. P. D. and Murphy, J. G.: Solubility and reactivity of HNCO
20 in water: insights into HNCO's fate in the atmosphere, Atmospheric Chem. Phys., 16(2), 703–714,
21 doi:10.5194/acp-16-703-2016, 2016b.

22 Brady, J. M., Crisp, T. A., Collier, S., Kuwayama, T., Forestieri, S. D., Perraud, V., Zhang, Q., Kleeman, M. J.,
23 Cappa, C. D. and Bertram, T. H.: Real-Time Emission Factor Measurements of Isocyanic Acid from Light Duty
24 Gasoline Vehicles, Environ. Sci. Technol., 48(19), 11405–11412, doi:10.1021/es504354p, 2014.

25 Büchler, H., Bühler, R. E. and Cooper, R.: Pulse radiolysis of aqueous cyanide solutions. Kinetics of the
26 transient hydroxyl radical and hydrogen atom adducts and subsequent rearrangements, J. Phys. Chem., 80(14),
27 1549–1553, doi:10.1021/j100555a006, 1976.

28 Bunkan, A. J. C., Mikoviny, T., Nielsen, C. J., Wisthaler, A. and Zhu, L.: Experimental and Theoretical Study
29 of the OH-Initiated Photo-oxidation of Formamide, J. Phys. Chem. A, 120(8), 1222–1230,
30 doi:10.1021/acs.jpca.6b00032, 2016.

31 Calvert, J. G.: Mechanisms of atmospheric oxidation of the alkanes, Oxford University Press, Oxford; New
32 York., 2008.

33 Chandra, B. P. and Sinha, V.: Contribution of post-harvest agricultural paddy residue fires in the NW Indo-
34 Gangetic Plain to ambient carcinogenic benzenoids, toxic isocyanic acid and carbon monoxide, Environ. Int.,
35 88, 187–197, doi:10.1016/j.envint.2015.12.025, 2016.

36 Criegee, R.: Mechanism of Ozonolysis, Angew. Chem. Int. Ed. Engl., 14(11), 745–752,
37 doi:10.1002/anie.197507451, 1975.

38 Crippa, M., Janssens-Maenhout, G., Dentener, F., Guizzardi, D., Sindelarova, K., Muntean, M., Van Dingenen,
39 R. and Granier, C.: Forty years of improvements in European air quality: regional policy-industry interactions
40 with global impacts, Atmospheric Chem. Phys., 16(6), 3825–3841, doi:10.5194/acp-16-3825-2016, 2016.

41 Dunning, T. H.: Gaussian basis sets for use in correlated molecular calculations. I. The atoms boron through
42 neon and hydrogen, J. Chem. Phys., 90(2), 1007–1023, doi:10.1063/1.456153, 1989.

https://doi.org/10.5194/acp-2019-1138
Preprint. Discussion started: 3 February 2020

Atmospheric Chemistry and Physics Discussions

Fenimore, C. P.: Formation of nitric oxide in premixed hydrocarbon flames, Proc. Combust. Inst., 13, 373–380, 1971.

Finlayson-Pitts, B. J. and Pitts, J. N.: Chemistry of the Upper and Lower Atmosphere: Theory, Experiments, and Applications, Academic Press, San Diego., 1999.

Forschungszentrum Jülich: JUWELS: Modular Tier-0/1 Supercomputer at Jülich Supercomputing Centre, J. Large-Scale Res. Facil., 5, A135, doi:10.17815/jlsrf-5-171, 2019.

Gardiner, W. C., Ed.: Gas-phase combustion chemistry, Springer, New York., 2000.

Heeb, N. V., Zimmerli, Y., Czerwinski, J., Schmid, P., Zennegg, M., Haag, R., Seiler, C., Wichser, A., Ulrich, A., Honegger, P., Zeyer, K., Emmenegger, L., Mosimann, T., Kasper, M. and Mayer, A.: Reactive nitrogen compounds (RNCs) in exhaust of advanced PM-NOx abatement technologies for future diesel applications, Atmos. Environ., 45(18), 3203–3209, doi:10.1016/j.atmosenv.2011.02.013, 2011.

Hems, R. F., Wang, C., Collins, D. B., Zhou, S. M., Borduas-Dedekind, N., Siegel, J. A. and Abbatt, J. P. D.: Sources of isocyanic acid (HNCO) indoors: a focus on cigarette smoke, Environ. Sci.-Process. Impacts, 21(8), 1334–1341, doi:10.1039/c9em00107g, 2019.

Hofzumahaus, A., Kraus, A., Kylling, A. and Zerefos, C. S.: Solar actinic radiation (280-420 nm) in the cloud-free troposphere between ground and 12 km altitude: Measurements and model results, J. Geophys. Res.-Atmospheres, 107(D18), doi:10.1029/2001jd900142, 2002.

Huber, K.-P. and Herzberg, G.: Molecular Spectra and Molecular Structure IV. Constants of diatomic molecules, Van Nostrand Reinhold, New York. [online] Available from: https://archive.org/details/MolecularSpectraAndMolecularStructureIV.ConstantsOfDiatomicMoleculesK.P.HuberG.Herzberg, 1979.

Jathar, S. H., Heppding, C., Link, M. F., Farmer, D. K., Akherati, A., Kleeman, M. J., de Gouw, J. A., Veres, P. R. and Roberts, J. M.: Investigating diesel engines as an atmospheric source of isocyanic acid in urban areas, Atmospheric Chem. Phys., 17(14), 8959–8970, doi:10.5194/acp-17-8959-2017, 2017.

Jöckel, P., Kerkweg, A., Pozzer, A., Sander, R., Tost, H., Riede, H., Baumgaertner, A., Gromov, S. and Kern, B.: Development cycle 2 of the Modular Earth Submodel System (MESSy2), Geosci. Model Dev., 3(2), 717–752, doi:10.5194/gmd-3-717-2010, 2010.

Johnston, H. S. and Heicklen, J.: Tunneling corrections for unsymmetrical Eckart potential energy barriers, J. Phys. Chem., 66(3), 532–533, doi:10.1021/j100809a040, 1962.

Kaiser, J. W., Heil, A., Andreae, M. O., Benedetti, A., Chubarova, N., Jones, L., Morcrette, J.-J., Razinger, M., Schultz, M. G., Suttie, M. and van der Werf, G. R.: Biomass burning emissions estimated with a global fire assimilation system based on observed fire radiative power, Biogeosciences, 9(1), 527–554, doi:10.5194/bg-9-527-2012, 2012.

Keller-Rudek, H., Moortgat, G. K., Sander, R. and Sorensen, R.: The MPI-Mainz UV/VIS Spectral Atlas of Gaseous Molecules of Atmospheric Interest, Earth Syst. Sci. Data, 5(2), 365–373, doi:10.5194/essd-5-365-2013, 2013.

Kerkweg, A., Sander, R., Tost, H. and Jöckel, P.: Technical note: Implementation of prescribed (OFFLEM), calculated (ONLEM), and pseudo-emissions (TNUDGE) of chemical species in the Modular Earth Submodel System (MESSy), Atmospheric Chem. Phys., 6(11), 3603–3609, doi:10.5194/acp-6-3603-2006, 2006.

Koss, A. R., Sekimoto, K., Gilman, J. B., Selimovic, V., Coggon, M. M., Zarzana, K. J., Yuan, B., Lerner, B. M., Brown, S. S., Jimenez, J. L., Krechmer, J., Roberts, J. M., Warneke, C., Yokelson, R. J. and de Gouw, J.: Non-methane organic gas emissions from biomass burning: identification, quantification, and emission factors from PTR-ToF during the FIREX 2016 laboratory experiment, Atmospheric Chem. Phys., 18(5), 3299–3319, doi:10.5194/acp-18-3299-2018, 2018.

https://doi.org/10.5194/acp-2019-1138
Preprint. Discussion started: 3 February 2020

Atmospheric Chemistry and Physics Discussions

Kumar, V., Chandra, B. P. and Sinha, V.: Large unexplained suite of chemically reactive compounds present in ambient air due to biomass fires, Sci. Rep., 8, 626, doi:10.1038/s41598-017-19139-3, 2018.

Le Picard, S. D., Tizniti, M., Canosa, A., Sims, I. R. and Smith, I. W. M.: The Thermodynamics of the Elusive HO_3 Radical, Science, 328(5983), 1258–1262, doi:10.1126/science.1184459, 2010.

Lee, C., Yang, W. and Parr, R. G.: Development of the Colle-Salvetti correlation-energy formula into a functional of the electron density, Phys. Rev. B, 37(2), 785–789, doi:10.1103/PhysRevB.37.785, 1988.

Leslie, M. D., Ridoli, M., Murphy, J. G. and Borduas-Dedekind, N.: Isocyanic acid (HNCO) and its fate in the atmosphere: a review, Environ. Sci.-Process. Impacts, 21(5), 793–808, doi:10.1039/c9em00003h, 2019.

Liebig, J. and Wöhler, F.: Untersuchungen über die Cyansäure, Ann. Phys., 96(11), 369–400, doi:10.1002/andp.18300961102, 1830.

Liggio, J., Stroud, C. A., Wentzell, J. J. B., Zhang, J. H., Sommers, J., Darlington, A., Liu, P. S. K., Moussa, S. G., Leithead, A., Hayden, K., Mittermeier, R. L., Staebler, R., Wolde, M. and Li, S. M.: Quantifying the Primary Emissions and Photochemical Formation of Isocyanic Acid Downwind of Oil Sands Operations, Environ. Sci. Technol., 51(24), 14462–14471, doi:10.1021/acs.est.7b04346, 2017.

Luo, Y.-R.: Comprehensive Handbook of Chemical Bond Energies, 0 ed., CRC Press., 2007.

Marcelino, N., Agundez, M., Cernicharo, J., Roueff, E. and Tafalla, M.: Discovery of the elusive radical NCO and confirmation of H_2NCO^+ in space, Astron. Astrophys., 612, L10, doi:10.1051/0004-6361/201833074, 2018.

Martin, J. M. L.: Ab initio total atomization energies of small molecules — towards the basis set limit, Chem. Phys. Lett., 259(5–6), 669–678, doi:10.1016/0009-2614(96)00898-6, 1996.

Mertens, J. D., Chang, A. Y., Hanson, R. K. and Bowman, C. T.: A Shock-Tube Study of Reactions of Atomic Oxygen with Isocyanic Acid, Int. J. Chem. Kinet., 24(3), 279–295, doi:10.1002/kin.550240306, 1992.

Nielsen, C. J., Herrmann, H. and Weller, C.: Atmospheric chemistry and environmental impact of the use of amines in carbon capture and storage (CCS), Chem. Soc. Rev., 41(19), 6684–6704, doi:10.1039/c2cs35059a, 2012.

Okabe, H.: Photodissociation of HNCO in Vacuum Ultraviolet - Production of NCO $A^2\Sigma$ and NH($A^3\pi$, πc^1), J. Chem. Phys., 53(9), 3507–3515, doi:10.1063/1.1674525, 1970.

Parandaman, A., Tangtartharakul, C. B., Kumar, M., Francisco, J. S. and Sinha, A.: A Computational Study Investigating the Energetics and Kinetics of the HNCO + $(CH_3)_2NH$ Reaction Catalyzed by a Single Water Molecule, J. Phys. Chem. A, 121(44), 8465–8473, doi:10.1021/acs.jpca.7b08657, 2017.

Pumphrey, H. C., Glatthor, N., Bernath, P. F., Boone, C. D., Hannigan, J. W., Ortega, I., Livesey, N. J. and Read, W. G.: MLS measurements of stratospheric hydrogen cyanide during the 2015-2016 El Niño event, Atmospheric Chem. Phys., 18(2), 691–703, doi:10.5194/acp-18-691-2018, 2018.

Purvis, G. D. and Bartlett, R. J.: A full coupled-cluster singles and doubles model: The inclusion of disconnected triples, J. Chem. Phys., 76(4), 1910, doi:10.1063/1.443164, 1982.

Roberts, J. M. and Liu, Y.: Solubility and solution-phase chemistry of isocyanic acid, methyl isocyanate, and cyanogen halides, Atmos Chem Phys, 19(7), 4419–4437, doi:10.5194/acp-19-4419-2019, 2019.

Roberts, J. M., Veres, P., Warneke, C., Neuman, J. A., Washenfelder, R. A., Brown, S. S., Baasandorj, M., Burkholder, J. B., Burling, I. R., Johnson, T. J., Yokelson, R. J. and de Gouw, J.: Measurement of HONO, HNCO, and other inorganic acids by negative-ion proton-transfer chemical-ionization mass spectrometry (NI-PT-CIMS): application to biomass burning emissions, Atmospheric Meas. Tech., 3(4), 981–990, doi:10.5194/amt-3-981-2010, 2010.

https://doi.org/10.5194/acp-2019-1138
Preprint. Discussion started: 3 February 2020

Atmospheric Chemistry and Physics Discussions

Roberts, J. M., Veres, P. R., Cochran, A. K., Warneke, C., Burling, I. R., Yokelson, R. J., Lerner, B., Gilman, J. B., Kuster, W. C., Fall, R. and de Gouw, J.: Isocyanic acid in the atmosphere and its possible link to smoke-related health effects, Proc. Natl. Acad. Sci. U. S. A., 108(22), 8966–8971, doi:10.1073/pnas.1103352108, 2011.

Roberts, J. M., Veres, P. R., VandenBoer, T. C., Warneke, C., Graus, M., Williams, E. J., Lefer, B., Brock, C. A., Bahreini, R., Ozturk, F., Middlebrook, A. M., Wagner, N. L., Dube, W. P. and de Gouw, J. A.: New insights into atmospheric sources and sinks of isocyanic acid, HNCO, from recent urban and regional observations, J. Geophys. Res.-Atmospheres, 119(2), 1060–1072, doi:10.1002/2013JD019931, 2014.

Roeckner, E., Brokopf, R., Esch, M., Giorgetta, M., Hagemann, S., Kornblueh, L., Manzini, E., Schlese, U. and Schulzweida, U.: Sensitivity of simulated climate to horizontal and vertical resolution in the ECHAM5 atmosphere model, J. Clim., 19(16), 3771–3791, doi:10.1175/JCLI3824.1, 2006.

Ruscic, B.: Uncertainty quantification in thermochemistry, benchmarking electronic structure computations, and Active Thermochemical Tables, Int. J. Quantum Chem., 114(17), 1097–1101, doi:10.1002/qua.24605, 2014.

Ruscic, B. and Bross, D. H.: Active Thermochemical Tables (ATcT) values based on ver. 1.122g of the Thermochemical Network (2019); available at ATcT.anl.gov, Argonne Natl. Lab. Act. Thermochem. Tables [online] Available from: http://atct.anl.gov/, 2019.

Ruscic, B., Wagner, A. F., Harding, L. B., Asher, R. L., Feller, D., Dixon, D. A., Peterson, K. A., Song, Y., Qian, X. M., Ng, C. Y., Liu, J. B. and Chen, W. W.: On the enthalpy of formation of hydroxyl radical and gas-phase bond dissociation energies of water and hydroxyl, J. Phys. Chem. A, 106(11), 2727–2747, doi:10.1021/jp013909s, 2002.

Sander, R., Baumgaertner, A., Gromov, S., Harder, H., Jöckel, P., Kerkweg, A., Kubistin, D., Regelin, E., Riede, H., Sandu, A., Taraborrelli, D., Tost, H. and Xie, Z.-Q.: The atmospheric chemistry box model CAABA/MECCA-3.0, Geosci. Model Dev., 4(2), 373–380, doi:10.5194/gmd-4-373-2011, 2011.

Sengupta, D. and Nguyen, M. T.: Mechanism of NH_2+CO_2 formation in OH+HNCO reaction: Rate constant evaluation via ab initio calculations and statistical theory, J. Chem. Phys., 106(23), 9703–9707, doi:10.1063/1.474090, 1997.

Sharpe, S. W., Johnson, T. J., Sams, R. L., Chu, P. M., Rhoderick, G. C. and Johnson, P. A.: Gas-phase databases for quantitative infrared spectroscopy, Appl. Spectrosc., 58(12), 1452–1461, doi:10.1366/0003702042641281, 2004.

Stone, D., Whalley, L. K. and Heard, D. E.: Tropospheric OH and HO_2 radicals: field measurements and model comparisons, Chem. Soc. Rev., 41(19), 6348–6404, doi:10.1039/c2cs35140d, 2012.

Suarez-Bertoa, R. and Astorga, C.: Isocyanic acid and ammonia in vehicle emissions, Transp. Res. Part -Transp. Environ., 49, 259–270, doi:10.1016/j.trd.2016.08.039, 2016.

SUVA: Grenzwerte am Arbeitsplatz 2016. [online] Available from: www.suva.ch/waswo, 2016.

SWEA: Swedish Work Environment Authority, Provisions and general recommendations on occupational exposure limit values, AFS 2011:18., 2011.

Taylor, W. D., Allston, T. D., Moscato, M. J., Fazekas, G. B., Kozlowski, R. and Takacs, G. A.: Atmospheric Photo-Dissociation Lifetimes for Nitromethane, Methyl Nitrite, and Methyl Nitrate, Int. J. Chem. Kinet., 12(4), 231–240, doi:10.1002/kin.550120404, 1980.

Tost, H., Jöckel, P., Kerkweg, A., Sander, R. and Lelieveld, J.: Technical note: A new comprehensive SCAVenging submodel for global atmospheric chemistry modelling, Atmospheric Chem. Phys., 6(3), 565–574, doi:10.5194/acp-6-565-2006, 2006.

Truhlar, D. G., Garrett, B. C. and Klippenstein, S. J.: Current Status of Transition-State Theory, J. Phys. Chem., 100(31), 12771–12800, doi:10.1021/jp953748q, 1996.

https://doi.org/10.5194/acp-2019-1138
Preprint. Discussion started: 3 February 2020

Atmospheric Chemistry and Physics Discussions

Tsang, W.: Chemical Kinetic Data Base for Propellant Combustion. II. Reactions Involving CN, NCO, and HNCO, J. Phys. Chem. Ref. Data, 21(4), 753, doi:10.1063/1.555914, 1992.

Tully, F. P., Perry, R. A., Thorne, L. R. and Allendorf, M. D.: Free-radical oxidation of isocyanic acid, Symp. Int. Combust., 22(1), 1101–1106, doi:10.1016/S0082-0784(89)80120-1, 1989.

Uno, K., Hikida, T., Hiraya, A. and Shobatake, K.: Formation of NH($C^1\Pi$), NH($A^3\Pi$) and NCO($A^2\Sigma$) in the VUV Photolysis of HNCO, Chem. Phys. Lett., 166(5–6), 475–479, doi:10.1016/0009-2614(90)87136-F, 1990.

Varandas, A. J. C.: Odd-Hydrogen: An Account on Electronic Structure, Kinetics, and Role of Water in Mediating Reactions with Atmospheric Ozone. Just a Catalyst or Far Beyond?, Int. J. Quantum Chem., 114(20), 1327–1349, doi:10.1002/qua.24580, 2014.

Vatsa, R. K. and Volpp, H. R.: Absorption cross-sections for some atmospherically important molecules at the H atom Lyman-alpha wavelength (121.567 nm), Chem. Phys. Lett., 340(3–4), 289–295, doi:10.1016/S0009-2614(01)00373-6, 2001.

Wang, Z., Nicholls, S. J., Rodriguez, E. R., Kummu, O., Horkko, S., Barnard, J., Reynolds, W. F., Topol, E. J., DiDonato, J. A. and Hazen, S. L.: Protein carbamylation links inflammation, smoking, uremia and atherogenesis, Nat. Med., 13(10), 1176–1184, doi:10.1038/nm1637, 2007.

Wentzell, J. J. B., Liggio, J., Li, S.-M., Vlasenko, A., Staebler, R., Lu, G., Poitras, M.-J., Chan, T. and Brook, J. R.: Measurements of Gas phase Acids in Diesel Exhaust: A Relevant Source of HNCO?, Environ. Sci. Technol., 47(14), 7663–7671, doi:10.1021/es401127j, 2013.

Wooldridge, M. S., Hanson, R. K. and Bowman, C. T.: A shock tube study of CO + OH → CO_2 + H and HNCO + OH → products via simultaneous laser adsorption measurements of OH and CO_2, Int. J. Chem. Kinet., 28(5), 361–372, doi:10.1002/(SICI)1097-4601(1996)28:5<361::AID-KIN5>3.0.CO;2-T, 1996.

Young, P. J., Emmons, L. K., Roberts, J. M., Lamarque, J.-F., Wiedinmyer, C., Veres, P. and VandenBoer, T. C.: Isocyanic acid in a global chemistry transport model: Tropospheric distribution, budget, and identification of regions with potential health impacts, J. Geophys. Res.-Atmospheres, 117, D10308, doi:10.1029/2011JD017393, 2012.

Zabardasti, A. and Solimannejad, M.: Theoretical study and AIM analysis of hydrogen bonded clusters of water and isocyanic acid, J. Mol. Struct.-Theochem, 819(1–3), 52–59, doi:10.1016/j.theochem.2007.05.032, 2007.

Zabardasti, A., Amani, S., Solimannejad, M. and Salehnassaj, M.: Theoretical study and atoms in molecule analysis of hydrogen bonded clusters of ammonia and isocyanic acid, Struct. Chem., 20(6), 1087–1092, doi:10.1007/s11224-009-9513-1, 2009.

Zabardasti, A., Kakanejadifard, A., Kikhaei, M. and Solimannejad, M.: Theoretical studies and topological analysis of the electron density of clusters of O_3 with HNCO and HCNO, J. Mol. Struct.-Theochem, 961(1–3), 1–5, doi:10.1016/j.theochem.2010.08.015, 2010.

Zhao, Y. and Truhlar, D. G.: The M06 suite of density functionals for main group thermochemistry, thermochemical kinetics, noncovalent interactions, excited states, and transition elements: two new functionals and systematic testing of four M06-class functionals and 12 other functionals, Theor. Chem. Acc., 120(1–3), 215–241, doi:10.1007/s00214-007-0310-x, 2008.